Front. Med. 2025, 19(6): 1163−1180
https://doi.org/10.1007/s11684-025-1173-z

RESEARCH ARTICLE

Endoplasmic reticulum stress upregulate HYOU1 and mediates lenvatinib resistance in liver cancer through ERK/MAPK pathway

Xiao Du[1], Weijia Jiang[1], Sitong Yan[1], Xiang Chen[1], Anqi Wang[1], Jiatao Liu[1,2], Lulu Fan[1], Yuhan Huang[1], Xiangyu Zu[1], Guoping Sun (✉)[1]

[1]*Department of Oncology, the First Affiliated Hospital of Anhui Medical University, Hefei 230000, China;* [2]*Department of Pharmacy, the First Affiliated Hospital of Anhui Medical University, Hefei 230000, China*

Abstract **Endoplasmic reticulum stress (ERS) is commonly observed in liver cancer and is associated with drug sensitivity. Consequently, ERS-related genes may serve as targets for enhancing treatment sensitivity. This study analyzed RNA and proteomic sequencing data from induced and non-induced ERS and identified hypoxia-upregulated protein 1 (HYOU1) as an ERS-related gene. We confirmed that ERS regulated HYOU1 expression. Database and microarray analyses revealed that HYOU1 expression level was significantly higher in cancer tissues than in normal tissues ($P < 0.05$). Additionally, HYOU1 upregulation correlated with poor clinical outcomes ($P < 0.05$). Findings from animal experiments, CCK-8 assays, colony formation assays, wound healing assays, transwell assays, and flow cytometry results showed that HYOU1 decreased the inhibition of cell proliferation, migration, invasion, and tumor growth while inducing apoptosis. Conversely, HYOU1 overexpression caused the opposite effects. Combining RNA-sequencing data from *HYOU1* knockdown and Western blot (WB) results, we have, for the first time, identified that HYOU1 activates the ERK/MAPK pathway. We show that ERS promotes resistance to lenvatinib, whereas HYOU1 knockdown increases sensitivity to lenvatinib. We believe that HYOU1 plays a crucial role in treating lenvatinib-resistant liver cancer.**

Keywords liver cancer; endoplasmic reticulum stress; HYOU1; lenvatinib; ERK/MAPK pathway

Introduction

Liver cancer poses a significant global health concern. As of 2020, it ranks sixth in incidence and third in mortality among cancers [1,2]. Development of the liver cancer is influenced by several risk factors, including chronic viral infections, tobacco use, excessive alcohol consumption, and non-alcoholic fatty liver disease. Prevention and early treatment can improve the efficiency of diagnosis and intervention. Nevertheless, liver cancer is most often detected at an advanced stage; therefore, most patients rely only on drug therapy for survival after diagnosis [3]. For advanced liver cancer, standard treatment strategies, including targeted therapies such as lenvatinib, offer only modest survival benefits, typically extending life by just 2 to 3 months, with a median overall survival (OS) of around one year. Importantly, acquired resistance to lenvatinib has been clearly shown to significantly diminish its therapeutic efficacy in the systemic treatment of liver cancer. Therefore, identifying new therapeutic targets for liver cancer and reducing treatment resistance are urgent issues that must be addressed.

The endoplasmic reticulum (ER) plays a critical role in ensuring the correct folding of newly synthesized peptides and proteins. ER homeostasis is disturbed when improperly folded or unfolded proteins accumulate in the cell, triggering a condition referred to as endoplasmic reticulum stress (ERS). During ERS, the unfolded protein response (UPR) is triggered to maintain homeostasis. However, prolonged and severe ERS exceeding the cell's adaptive capacity can lead to cell death [4]. ERS is involved in the progression of various diseases (including inflammatory disorders, immune system dysfunction, and cancers) and drug resistance. Following ERS, the UPR is activated, contributing to chemotherapy resistance [5]. Persistent conditions such as ischemia, hypoxia, and nutrient deprivation often lead to chronic and sustained

Received May 8, 2025; accepted August 14, 2025
Correspondence: Guoping Sun, sungp@ahmu.edu.cn

ERS in the tumor microenvironment. This may be related to poor therapeutic outcomes observed in patients with advanced liver cancer.

Hypoxia-upregulated protein 1 (HYOU1) is a member of the HSP70 family of heat shock proteins. It was initially discovered in hypoxic astrocytes in mice, and one study showed that HYOU1 maintained the viability of neuronal cells under stress [6]. Exhibiting cytoprotective effects, HYOU1 functions under renal, neurological, and cardiovascular hypoxia [7,8]. HYOU1 expression is elevated in various cancers and has been found to prompt tumorigenesis and progression of breast cancer, nasopharyngeal carcinoma, bladder cancer, and other malignancies [9–11]. A previous study has indicated that HYOU1 is associated with angiogenesis [12]. By targeting vascular endothelial growth factor receptors 1 through 3 (VEGFR1-3), as well as RET and KIT, lenvatinib effectively suppresses tumor cell proliferation and the formation of new blood vessels [13]. We hypothesized that HYOU1 influences lenvatinib resistance in liver cancer. Studies have shown that the MAPK pathway can be regulated by ERS and that abnormal activation of the MAPK pathway has been associated with lenvatinib resistance [14,15]. We further explored the ERS-mediated regulation of HYOU1, the role of HYOU1 in liver cancer, its influence on lenvatinib resistance, and the involvement of the MAPK pathway in these processes.

Materials and methods

Patient samples

A total of 83 hepatocellular carcinoma (HCC) tissue samples were obtained from patients admitted to the First Affiliated Hospital of Anhui Medical University (2020–2024). The selection of HCC cases was based on specific inclusion and exclusion criteria, as outlined below: (1) pathological diagnosis confirms primary liver cancer; (2) the patient has no history of other types of malignant tumors; (3) the patient has undergone curative surgical resection for liver cancer; (4) before surgical intervention, patients had not undergone radiotherapy, chemotherapy, or any other form of treatment; (5) the collected tissue specimens were accompanied by comprehensive clinical data. Patients gave written informed consent prior to participation. The study protocol received ethical approval from the Ethics Committee of Anhui Medical University. Additionally, four matched pairs of HCC and adjacent non-tumorous liver tissue were collected from the same institution.

Reagents

Lenvatinib (E7080) was purchased from MedChemExpress (MCE). Tunicamycin (TM, Cat#T7080), an ERS inducer, and 4-phenylbutyric acid (4PBA, Cat#IP5000), an ERS inhibitor, were obtained from Solarbio. U0126 (Cat#GC45099), an ERK1/2 inhibitor, was purchased from GLPBio.

Cell culture

The Shanghai Cell Bank of the Chinese Academy of Sciences provided HepG2, Hep3B, HCCLM3, MHCC97h, and Huh7 cell lines (Cat#SCSP-510, SCSP-5045, SCSP-5092, SCSP-5093, and SCSP-526). The cells underwent mycoplasma testing and short-tandem repeat profiling. Cells were cultured in DMEM (Wisent, China), supplemented with penicillin-streptomycin solution (Beyotime, China) and 10% fetal bovine serum (Wisent, China), in a 5% CO_2 incubator at 37 °C.

Plasmid transfection and small interfering RNA (siRNA)

The *HYOU1* overexpression plasmid was constructed by the GENE Company, and Lipo3000 (Invitrogen, USA) was used to introduce it into cells following the manufacturer's guidelines. GenePharma (Shanghai, China) provided the siRNA fragments designed to target *HYOU1* and negative control sequences. *CALNP* RNAi (D-nano Therapeutics, Beijing, China) was used to transfect *HYOU1* following the supplier's protocol. The sequences are provided in Table S1.

Lentiviral infection

The seeded cells were cultured for 24 h before adding the lentiviral vector and the transfection reagent, polybrene. The medium was changed 24 h later, and puromycin (Biosharp, China) was added at the appropriate concentration 48 h post-infection to select and maintain the cells.

CCK-8 assay

Overall, 2000–3000 cells were seeded in each well of a 96-well plate. A mixture of CCK-8 (Biosharp, China) and complete culture medium was added at a 1:9 ratio after 24 h of culture. The cells were incubated at 37 °C for 0.5–1 h. Absorbance was measured at 450 nm to calculate the proliferation efficiency. To measure the cytotoxicity, 5000–10 000 cells were seeded in each well, and after adding the drug for a certain period, the absorbance was measured.

Cell colony formation assay

Overall, 400–1000 cells were seeded per well in 6-well

plates. After a 14-day incubation, the cells were treated with 4% formaldehyde and stained with crystal violet. Images were captured and the number of colonies was recorded.

Wound healing assay

The cells were seeded in a 6-well plate, and once they reached confluence, a scratch was made across the bottom of each well. Serum-free medium was added after washing with PBS. Before capturing the images under a microscope, the cells were cultured for 0, 24, and 48 h.

Transwell assay

In the bottom of the Transwell insert, 600 μL of culture medium supplemented with 20% serum was added in advance. After 24 h of starvation, the cells were digested and resuspended, and then 200 μL of the resulting suspension was introduced into the upper chamber for migration or invasion analysis. For the invasion assay, the upper chamber was pre-coated with Matrigel diluted at a ratio of 1:8 prior to the introduction of cells. Following an incubation period of 24 h for migration assays and 48 h for invasion assays, the cells were fixed using formaldehyde, stained with crystal violet, and visualized under a microscope.

RNA extraction and RT-qPCR

Total RNA was isolated using TRIzol reagent (Invitrogen, USA), after which cDNA was generated through reverse transcription employing the Vazyme kit (R222, China). Using the ChamQ Universal SYBR qPCR Master Mix (Vazyme, #Q711, China) to carry out quantitative real-time PCR. The thermal cycling protocol consisted of an initial denaturation at 95 °C for 0.5 min (single cycle), followed by 40 cycles of 95 °C for 10 s and 60 °C for 0.5 min. The primer sequences used in this analysis are provided in Table S2.

Protein extraction and Western blotting (WB) experiment

A pre-cooled protein lysis buffer was applied at a ratio of 100 μL per 5×10^5 cells and incubated on ice for 0.5 h. A standard protein solution (1 mg/mL) was prepared in PBS. The bicinchoninic acid (BCA) working reagent (Beyotime, China) was formulated by combining BCA reagents A and B in a 50:1 ratio. This working solution was then added to tubes containing both protein samples and standards, and incubation was carried out at 37 °C for 0.5 h. The absorbance was recorded at 562 nm to generate a standard curve. The resulting solution was utilized to quantify protein levels. An equal amount of protein (20 μg per sample) was resolved by SDS-PAGE and then transferred to a PVDF membrane. The membrane was incubated overnight at 4 °C with the primary antibody following a blocking step. Afterward, it was exposed to the secondary antibody for 1 h at ambient temperature and protein bands were detected. As internal loading controls, β-actin, GAPDH, and β-tubulin were used, with details regarding antibody sources and dilution ratios provided in Table S3.

Flow cytometry

To assess apoptosis in liver cancer cells under different treatment conditions, flow cytometry was performed. When the liver cancer cells in the 6-well plate reached 80%–90% confluence, the adherent cells were digested with trypsin solution without EDTA (Beyotime, China) and collected using centrifugation before being twice resuspended in PBS. Next, 1 mL of Annexin V binding solution was added to 1×10^6 cells and the cells were resuspended, followed by the addition of 5 μL Annexin-FITC and 5 μL PI solution (BestBio, China). The cells were then incubated in the dark at 2–8 °C for 15 min and an additional 5 min. Apoptosis was assessed using flow cytometry (CytoFLEX).

RNA sequencing (RNA-seq)

To investigate the gene expression differences after TM treatment and *HYOU1* knockdown, we performed RNA-seq separately for each condition. Each group included three replicate samples during sample preparation. RNA samples for sequencing were extracted using TRIzol reagent, and their quality was verified using an Agilent 2100 Bioanalyzer. Oligo-dT magnetic beads were used to enrich mRNA from total RNA. The isolated mRNA was fragmented using a fragmentation buffer and subsequently used for library preparation. Initial library quantification was conducted with a Qubit 2.0 fluorometer, and the insert size was assessed using an Agilent 2100 Bioanalyzer. The effective concentration of the library was determined by performing qRT-PCR. The samples that met the quality criteria were subjected to Illumina sequencing (Illumina NovaSeq 6000) to generate transcriptomic data. Quantitative analysis of the transcriptomic data was performed using the featureCounts tool from the Subread software package.

TMT-based quantitative proteomics analysis

HepG2 cells were pretreated with TM to establish an *in vitro* ERS model, and the blank control group HepG2 cells were used for protein extraction using RIPA buffer. Each group included three replicate samples. After quantification using BCA, proteins were precipitated

using acetone. The protein samples were then resuspended in a protein resuspension solution, and dithiothreitol and iodoacetamide solutions were added for resolubilization, reduction, and alkylation of the proteins. After digestion with trypsin, the samples were incubated at 37 °C with shaking overnight. TMT labeling (Thermo Fisher TMT) was performed in accordance with the manufacturer's instructions. Trifluoroacetic acid was added to precipitate the peptides, which were desalted and separated under alkaline conditions. The peptides prepared by the above method were separated using a nano-UPLC system (nanoElute2, Bruker, Germany), and data were collected using a mass spectrometer (timsTOF Pro2, Bruker, Germany) equipped with a nanospray ion source. The raw data files were analyzed using the SpectroMine software (version 4.1.230421.52329; Biognosys AG) with the Pulsar search engine for database searching, followed by qualitative analysis after the search was completed.

Animal experiments

BALB/c nude mice aged 3–4 weeks were obtained from Jiangsu Jicui Pharmaceutical Co., Ltd. (Nanjing, China) and assigned to experimental groups through randomization. *HYOU1*-deficient Hep3B cells and their control counterparts were suspended in 100 μL of DMEM (2×10^6 cells) and injected subcutaneously into the mice's right axillary region. Tumor dimensions were recorded at 5-day intervals. After a 20-day observation period, mice were sacrificed using CO_2 exposure, and both tumor size and mass were evaluated.

In the lenvatinib administration experiment, treatment commenced once tumor volumes reached approximately 100 mm^3, with oral gavage of lenvatinib at a dose of 10 mg/kg. Lenvatinib was formulated by suspending 2 mg of the compound in 1 mL of 0.5% methylcellulose solution. Tumor progression was monitored every 5 days. Following 21 days of drug exposure, mice were euthanized using CO_2, and tumor parameters were documented. Investigators performing outcome assessments were blinded to group assignments. This study received ethical approval from the Animal Ethics Committee of Anhui Medical University (No. 20242232).

Immunohistochemistry (IHC)

To detect the expression of specific antigens in tissues or cells, immunohistochemistry was performed. Tissue sections designated for staining were first baked in an oven for 2–3 h, followed by deparaffinization in xylene and rehydration through a graded series of ethanol solutions. Antigen retrieval was then conducted using a buffer suitable for the specific antibody, applying microwave-assisted gradual heating. Endogenous peroxidase activity was neutralized with a blocking solution. At room temperature, non-specific binding was blocked by incubating slides with goat serum for 0.5 h. Afterward, they were exposed to the primary antibody solution overnight at a temperature of 2–8 °C. The next day, incubation with the secondary antibody was carried out at 37 °C. Color development was performed using DAB, and nuclei were subsequently counterstained with hematoxylin. Slides underwent dehydration through a reverse ethanol gradient, cleared in xylene, and allowed to air dry before coverslip mounting.

For immunohistochemical evaluation, scores were calculated by multiplying the percentage of positively stained cells (0, none; 1, ⩽ 25%; 2, 26%–50%; 3, 51%–75%; 4, > 75%) by the staining intensity (0, negative; 1, light yellow; 2, yellowish brown; 3, deep brown). A composite score exceeding 5 denoted high expression, whereas a score below 5 was considered indicative of low expression.

Hematoxylin and eosin (HE) staining

To visualize tissue or cellular structures for observation and analysis, HE staining was performed. The tissue samples were immersed in xylene for deparaffinization, followed by hydration with successive concentrations of ethanol and washing with PBS. The samples were stained with hematoxylin, differentiated in 1% hydrochloric acid-ethanol, and counterstained with a weak alkaline blue solution. The samples were then washed with distilled water and stained with eosin. After sequential dehydration using a gradient ethanol solution, the samples were treated with xylene and sealed with a neutral resin for microscopic imaging and analysis.

Statistical analysis

GraphPad Prism version 8.0 was used to carry out statistical analyses. Prior to performing hypothesis testing, data sets were evaluated for normality and homogeneity of variances. Shapiro–Wilk test was used to assess normal distribution, while Levene's test was employed to verify variance homogeneity. If both assumptions were satisfied, differences between two independent groups were analyzed using an unpaired, two-tailed Student's *t*-test. For comparisons involving more than two groups, either one-way or two-way ANOVA was selected based on the experimental design. Quantitative data were generally presented as mean ± standard deviation (SD) unless stated otherwise. Pearson correlation analysis was used to determine relationships between variables. OS in relation to HYOU1 expression levels was assessed using Kaplan–Meier survival analysis, while statistical significance between survival curves was evaluated using the Log-rank test.

Associations between HYOU1 expression and clinicopathological features were evaluated using either the chi-square test or the rank-sum test, as appropriate. *In vivo* experiments involved groups of 5 mice, randomly allocated. Differences in tumor weights from subcutaneous tumor formation and drug treatment studies were assessed using an unpaired two-tailed *t*-test or one-way ANOVA, respectively. Tumor volume data were analyzed using two-way ANOVA. Each experiment was conducted with at least three independent biological replicates. Significance was set as $P < 0.05$.

Results

HYOU1 is elevated in liver cancer and correlated with unfavorable prognosis

To investigate the effect of ERS on liver cancer progression, we established an ERS model in liver cancer cells treated with TM (each group included 3 replicate samples). We used high-throughput RNA-seq and LC-MS/MS proteomic analysis to evaluate the effects of ERS on transcriptional and proteomic alterations in liver cancer cells. RNA sequencing revealed a total of 1061 genes exhibiting significant differential expression ($|\log_2$FC (fold change)$| \geqslant 1$, $P \leqslant 0.05$) after induction of ERS, comprising 601 genes with increased expression and 460 with decreased expression (Fig. 1A). In parallel, proteomic profiling identified 120 proteins with altered expression levels, of which 75 were upregulated and 45 were downregulated (Fig. 1B).

Intersection analysis between the upregulated target proteins of DEGs identified in RNA-seq and the upregulated proteins from proteomic analysis identified 20 ERS-specific proteins (Table S4). Seven molecules (AGPAT4, HSPA5, HYOU1, MANF, ASNS, SSR2, and LONP1) were differentially expressed between liver cancer and adjacent tissues and were associated with clinical prognosis. qPCR confirmed that their expression levels were elevated after TM treatment (Fig. 1C). AGPAT4 expression was detected only in the TM group; therefore, it was excluded from further investigation. HSPA5-encoded glucose-regulated protein 78 (GRP78) is a well-established ERS marker. HYOU1 exhibited the most significant differential expression among the remaining proteins, making it the primary focus of subsequent research (Fig. 1D).

Additional examination of the TCGA-LIHC data set indicated a notable increase in HYOU1 expression in liver cancer tissues (Fig. 1E). Data from the TIMER database also indicated HYOU1 upregulation in multiple cancer types, including liver cancer (Fig. 1F). IHC staining was conducted on tissue specimens from 83 HCC patients, obtained between 2020 and 2024 at the First Affiliated Hospital of Anhui Medical University. The analysis revealed a marked elevation in HYOU1 expression within tumor tissues relative to the corresponding adjacent non-tumorous samples (Fig. 1G and 1H).

In addition, freshly collected tumor tissues along with matched adjacent normal samples from 4 individuals diagnosed with HCC were subjected to WB analysis. The results demonstrated an increase in HYOU1 protein levels in the tumor specimens compared to the non-tumorous counterparts (Fig. 1I). We examined data from the Gene Expression Profiling Interactive Analysis (GEPIA) database to investigate the relationship between HYOU1 expression and patient survival (Fig. 1J). We found that patients with high HYOU1 expression had reduced OS ($P = 0.021$). The late-stage crossing of curves may reflect statistical variability or survivor bias, rather than a true reversal of risk. Therefore, HYOU1 expression appears to be associated with poor prognosis primarily during the early disease course in HCC. Similar results were obtained when analyzing the survival data of 29 patients with HCC in our study cohort ($P < 0.01$) (Fig. 1K).

Additionally, we investigated the relationship between HYOU1 expression levels and various clinicopathological parameters in a cohort of 83 HCC patients. The analysis revealed a statistically significant correlation between HYOU1 expression and tumor stage ($P = 0.039$). However, no meaningful associations were found with patient age, gender, history of hepatitis or cirrhosis, AFP level, or tumor size (Table 1).

ERS activation upregulates HYOU1 expression in liver cancer cells

To investigate the link between ERS and HYOU1 expression, HepG2 cells were treated with varying concentrations of TM. WB and qRT-PCR analyses demonstrated a dose-dependent elevation in HYOU1 and GRP78 expression (GRP78: 0 μmol/L : 0.625 μmol/L = (0.44 ± 0.13) : (0.85 ± 0.05), $P < 0.01$; 0 μmol/L : 1.25 μmol/L = (0.44 ± 0.13) : (1.12 ± 0.08), $P < 0.01$; 0 μmol/L : 2.5 μmol/L = (0.44 ± 0.13) : (1.21 ± 0.17), $P < 0.01$; 0 μmol/L : 5 μmol/L = (0.44 ± 0.13) : (1.30 ± 0.21), $P < 0.01$. HYOU1: 0 μmol/L : 0.625 μmol/L = (0.42 ± 0.09) : (0.88 ± 0.07), $P < 0.01$; 0 μmol/L : 1.25 μmol/L = (0.44 ± 0.13) : (1.19 ± 0.13), $P < 0.01$; 0 μmol/L : 2.5 μmol/L = (0.44 ± 0.13) : (1.29 ± 0.11), $P < 0.01$; 0 μmol/L : 5 μmol/L = (0.44 ± 0.13) : (1.46 ± 0.01), $P < 0.01$) (Fig. 2A and 2B). Conversely, treatment with increasing concentrations of the ERS inhibitor 4-phenylbutyric acid (4-PBA) led to a progressive reduction in HYOU1 and GRP78 expression (GRP78: 0 mmol/L : 0.5 mmol/L = (1.27 ± 0.23) : (1.22 ± 0.02), *P*: ns; 0 mmol/L : 1 mmol/L = (1.27 ± 0.23) : (1.08 ± 0.00), $P < 0.01$; 0 mmol/L : 2 mmol/L = (1.27 ± 0.23) : (0.80 ± 0.09), $P < 0.01$; 0 mmol/L : 4 mmol/L = (1.27 ± 0.23) :

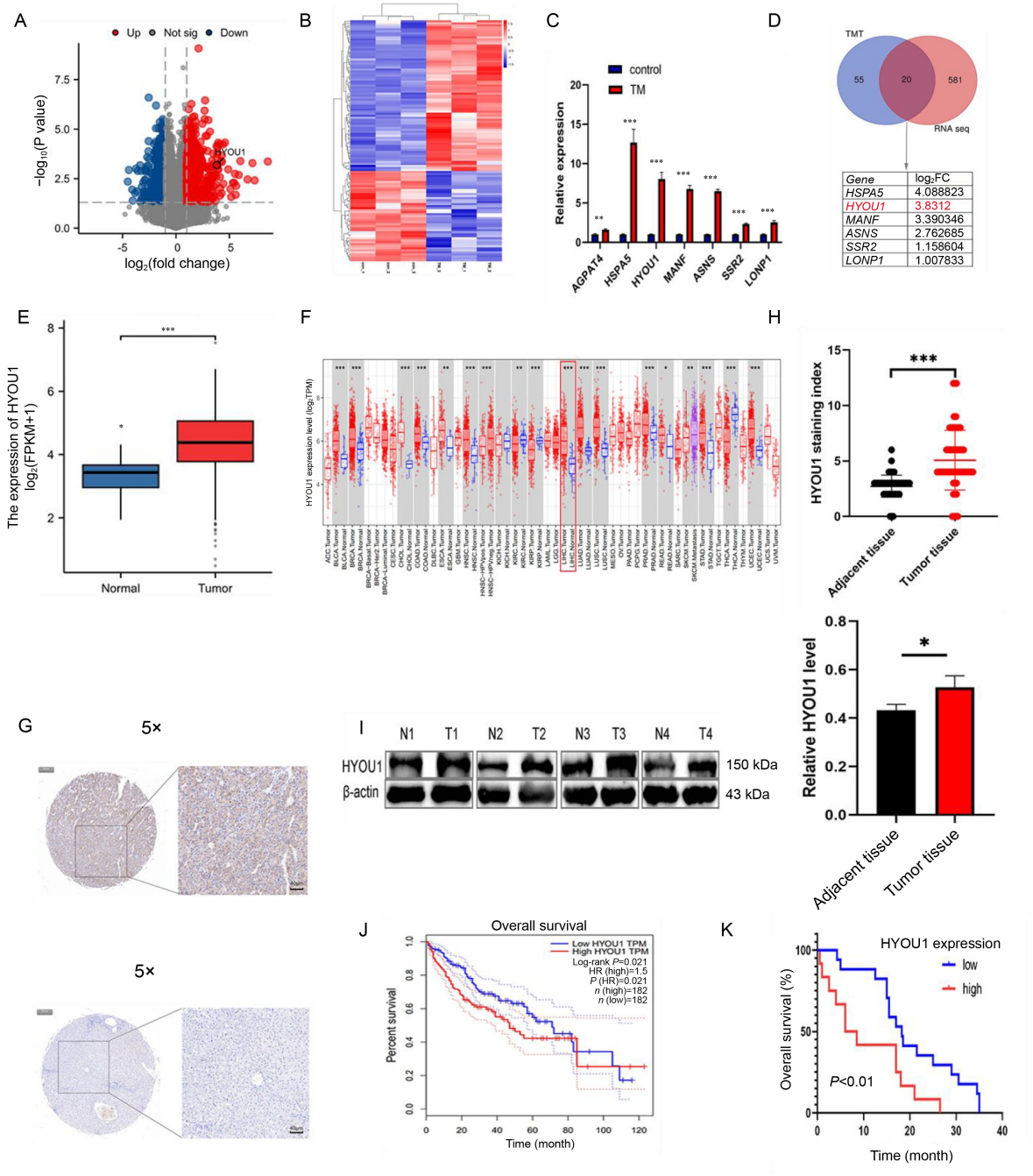

Fig. 1 HYOU1 is upregulated in liver cancer and correlates with poor prognosis. (A) Volcano plot illustrating DEGs identified through RNA-seq following TM treatment. (B) Heatmap depicting differentially expressed proteins derived from proteomic sequencing. (C) qPCR detecting mRNA expression of 7 molecules after TM treatment. (D) Venn diagram highlighting overlapping upregulated proteins from both sequencing. (E) TCGA data reveals elevated HYOU1 expression in liver cancer tissues. (F) Timer database indicates differential HYOU1 expression across various cancer types. (G) Representative IHC staining images (5×) showing distinct HYOU1 expression patterns in liver cancer tissues and adjacent tissues (scale bar: 40 μm). (H) IHC staining of HYOU1 in liver cancer tissues compared to adjacent normal tissues. (I) WB and quantitative evaluation of HYOU1 expression in 4 pairs of liver cancer tissues and adjacent tissues. (J) GEPIA data analysis examining the correlation between HYOU1 expression and OS. (K) Kaplan–Meier survival analysis for 29 liver cancer patients, categorized based on high or low HYOU1 expression levels. IHC, immunohistochemistry; WB, Western blotting. Statistical significance: $^{*}P < 0.05$, $^{**}P < 0.01$, $^{***}P < 0.001$.

(0.61 ± 0.05), $P < 0.01$. HYOU1: 0 mmol/L : 0.5 mmol/L = (1.29 ± 0.06) : (1.15 ± 0.02), P: ns; 0 mmol/L : 1 mmol/L = (1.29 ± 0.06) : (0.97 ± 0.02), $P < 0.01$; 0 mmol/L : 2 mmol/L = (1.29 ± 0.06) : (0.69 ± 0.07), $P < 0.01$; 0 mmol/L : 4 mmol/L = (1.29 ± 0.06) : (0.65 ± 0.07), $P < 0.01$) (Fig. 2C and 2D). The ERS induction model and inhibition model were established by stimulation with 2.5 μmol/L TM and 1 mmol/L 4-PBA, respectively. To

Table 1 Relationship between HYOU1 expression level and clinical characteristics of HCC patients

Clinical features	Number	HYOU1			Positive rate (%)	Z/χ^2	*P*
		Negative	Low	High			
Sex						3.25	0.197
Male	64	3	30	31	95.3		
Female	19	2	12	5	89.5		
Age						0.634	0.728
< 60 years	53	4	26	23	92.5		
⩾ 60 years	30	1	16	13	96.7		
History of hepatitis						1.815	0.404
Positive	61	3	29	29	95.1		
Negative	22	2	13	7	95.2		
History of cirrhosis						0.05	0.975
Positive	37	2	19	16	94.6		
Negative	46	3	23	20	93.5		
AFP						4.912	0.296
Low	32	2	20	10	93.8		
Middle	23	1	8	14	95.7		
High	28	2	14	12	92.9		
Stage						6.509	0.039
Phase 1–2	66	3	38	25	95.5		
Phase 3–4	17	2	4	11	88.2		
Tumor size						6.436	0.169
< 5 cm	30	2	20	8	93.3		
5–10 cm	37	2	17	18	94.6		
⩾ 10 cm	16	1	5	10	93.75		
Differentiation						0.76	0.944
High	27	2	15	10	92.6		
Middle	41	2	20	19	95.1		
Low	15	1	7	7	93.3		

further explore the correlation between ERS and HYOU1 expression, TM-induced ERS was inhibited using 4-PBA. The results showed that following the 4-PBA treatment, the expression levels of HYOU1 and GRP78 were significantly reduced compared to those in the ERS-induced group (GRP78: con : TM = (0.76 ± 0.13) : (1.19 ± 0.21), $P < 0.01$; TM : (TM + 4PBA) = (1.19 ± 0.21) : (0.75 ± 0.13), $P < 0.01$. HYOU1: con : TM = (0.52 ± 0.17) : (1.15 ± 0.02), $P < 0.01$; TM : (TM + 4PBA) = (1.15 ± 0.02) : (0.78 ± 0.14), $P < 0.01$) (Fig. 2E and 2F). Moreover, bioinformatics analysis using the TCGA database demonstrated a positive correlation between HYOU1 expression and key downstream ERS-related genes, including *HSPA5*, *ERN1*, *EIF2AK3*, *ATF4*, and *ATF6* (Fig. 2G).

We then assessed the expression of HYOU1 protein across different liver cancer cell lines. The findings revealed that HYOU1 expression was elevated in HepG2 and Hep3B cells, whereas it was comparatively lower in MHCC97H cells (Fig. 2H). To further investigate the functional role of HYOU1, we transfected HepG2 and Hep3B cells with specific siRNAs targeting HYOU1. Among the siRNA fragments tested, S1 exhibited stable and efficient HYOU1 knockdown at both the protein and mRNA levels in HepG2 (si-NC : si-S1 = (0.94 ± 0.07) : (0.11 ± 0.03), $P < 0.01$) (Fig. 2I and 2J) and Hep3B (si-NC : si-S1 = (0.88 ± 0.05) : (0.36 ± 0.03), $P < 0.01$) cells (Fig. 2K and 2L). Consequently, S1 was selected for the subsequent experiments.

HYOU1 upregulation enhances liver cancer cell growth while suppressing apoptosis

To investigate whether ERS promotes liver cancer progression by upregulating HYOU1, we silenced *HYOU1* expression in HepG2 cells using shRNA and

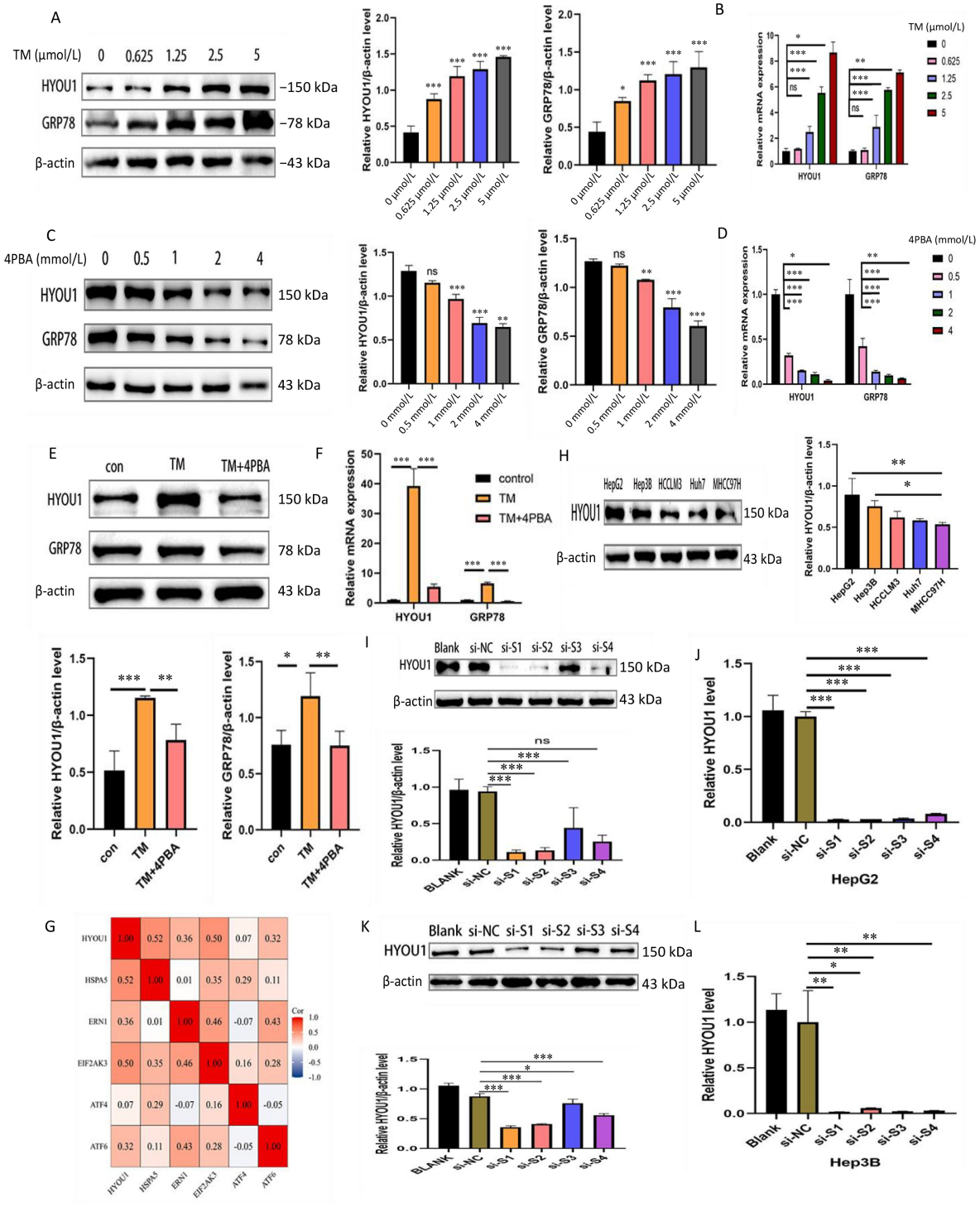

Fig. 2 ERS upregulates HYOU1 expression. The protein and mRNA levels of GRP78 and HYOU1 after treatment with increasing concentrations of (A, B) TM and (C, D) 4PBA. (E) Protein and (F) mRNA levels of GRP78 and HYOU1 in liver cancer cells stimulated with TM (2.5 μmol/L) alone or combined with 4PBA (1 mmol/L). (G) Correlation analysis between HYOU1 and genes downstream of ERS using TCGA-LIHC mRNA data. (H) HYOU1 expression and quantitative analysis in 5 liver cancer cell lines. Protein and mRNA expression of HYOU1 in (I, J) HepG2 and (K, L) Hep3B cells after siRNA knockdown. Statistical significance: $^{*}P < 0.05$, $^{**}P < 0.01$, $^{***}P < 0.001$.

assessed its effect on tumor cell vitality and proliferation using CCK-8 and colony formation assays. These findings indicated that silencing *HYOU1* inhibited the vitality and proliferation of HepG2 cells (Fig. 3A and 3B). A similar reduction in proliferation was observed in Hep3B cells following *HYOU*1 knockdown (Fig. 3C and 3D). Additionally, *in vivo* experiments showed that reducing HYOU1 expression led to a marked reduction in

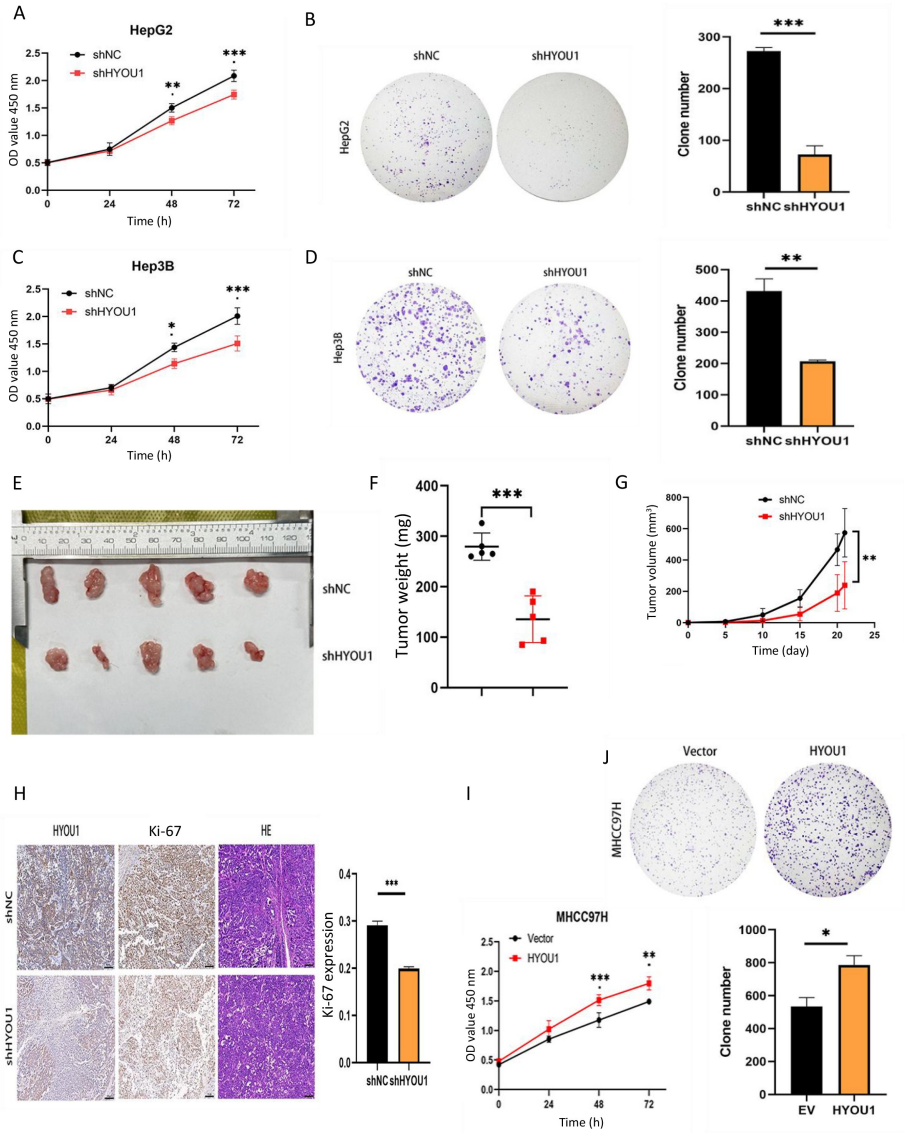

Fig. 3 HYOU1 promotes liver cancer cell proliferation. (A, B) In HepG2 cells, CCK-8 and colony formation assays are conducted to evaluate *HYOU1* knockdown effect on the vitality and proliferation. (C, D) In Hep3B cells, CCK-8 and colony formation assays are performed to examine *HYOU1* knockdown effect on vitality and proliferation. (E) Representative images of xenograft tumors from mice in both the shNC and shHYOU1 groups. (F, G) Tumor weight and volume measurements. (H) Immunohistochemistry staining of HYOU1 and Ki-67 expression (scale bar: 100 μm). (I, J) In MHCC97H cell, CCK-8 and colony formation assays are performed to assess the influence of HYOU1 overexpression on cell vitality and proliferation. Statistical significance: * $P < 0.05$; ** $P < 0.01$; *** $P < 0.001$.

tumor growth in mice (Fig. 3E). In the HYOU1 knockdown group, tumors were considerably smaller in both weight ($P < 0.01$) (Fig. 3F) and volume ($P < 0.01$) (Fig. 3G) compared to those in the control group. IHC analysis revealed that the proliferation marker Ki-67 was reduced in tumors with HYOU1 knockdown (Fig. 3H). Conversely, HYOU1 overexpression in MHCC97H cells enhanced liver cancer cell vitality and proliferation, as evidenced using the CCK-8 ($P < 0.01$) and colony formation assays ($P < 0.05$) (Fig. 3I and 3J).

Next, we investigated the effect of HYOU1 expression on apoptosis through WB and flow cytometry. These findings indicated that silencing HYOU1 enhanced apoptosis in HepG2 and Hep3B cells ($P < 0.01$) (Fig. 4A). WB analysis demonstrated that silencing HYOU1 led to an increase in Bax while reducing the levels of Bcl-2 (Fig. 4B and 4C) in HepG2 and Hep3B cells. In contrast, HYOU1 overexpression significantly reduced apoptosis, as demonstrated using flow cytometry ($P < 0.01$) (Fig. 4D). WB results further confirmed that HYOU1 overexpression significantly decreased Bax protein levels and increased Bcl-2 expression compared to the control group (Fig. 4E).

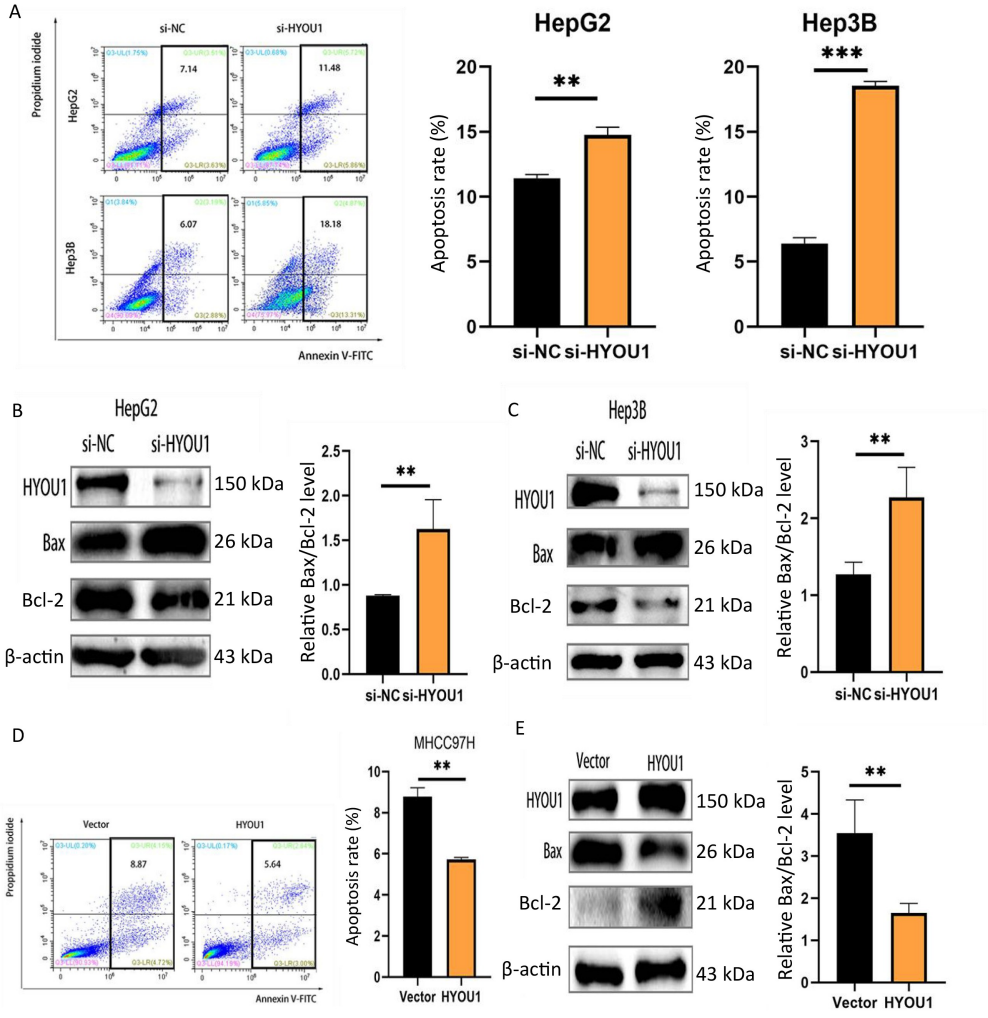

Fig. 4 HYOU1 inhibits liver cancer cell apoptosis. (A) Flow cytometry analysis demonstrating that *HYOU1* knockdown promotes apoptosis in HepG2 and Hep3B cells. (B, C) Detecting Bax and Bcl2 protein expression after HYOU1 knockdown in HepG2 and Hep3B cells by WB assay. (D) Flow cytometry analysis shows that HYOU1 overexpression inhibits apoptosis in MHCC97H cells. (E) WB analysis of Bax and Bcl-2 protein expression following HYOU1 overexpression. WB, Western blotting. Statistical significance: $^{*}P < 0.05$, $^{**}P < 0.01$, $^{***}P < 0.001$.

HYOU1 promotes migration and invasion of liver cancer cells

To explore the link between HYOU1 expression and the migratory and invasive properties of liver cancer cells, we knocked down *HYOU1* in HepG2 and Hep3B cells using shRNAs. Results from both Transwell and wound healing assays showed that HYOU1 silencing reduced HepG2 cells's migratory and invasive capabilities (Fig. 5A and 5B). Comparable findings were observed in Hep3B cells, where HYOU1 knockdown also suppressed migration and invasion (Fig. 5C and 5D). N-cadherin and vimentin are crucial markers of epithelial-mesenchymal transition (EMT), and their downregulation suggests a decrease in metastatic potential. In this context, silencing HYOU1 led to a significant reduction in N-cadherin and vimentin expression in both HepG2 and Hep3B cells, implying a potential suppression of their metastatic capacity (Fig. 5E and 5F). Overexpression of HYOU1 in MHCC97H cells increased migration and invasion, as demonstrated by both Transwell and wound healing assays (Fig. 5G and 5H). Furthermore, HYOU1 overexpression elevated the levels of N-cadherin and vimentin, suggesting an enhancement of metastatic potential in MHCC97H cells (Fig. 5I).

HYOU1 activates the ERK/MAPK pathway to mediate its biological functions in liver cancer cells

To investigate the mechanisms by which HYOU1 facilitates liver cancer cell growth, enhances migration and invasion, and suppresses apoptosis, we established HYOU1-knockdown Hep3B cells using lentiviral transduction and performed RNA-seq analysis. The results showed there were 1425 DEGs after *HYOU1* inhibition ($|\log_2 FC| \geqslant 1$, $P \leqslant 0.05$), with 794 genes

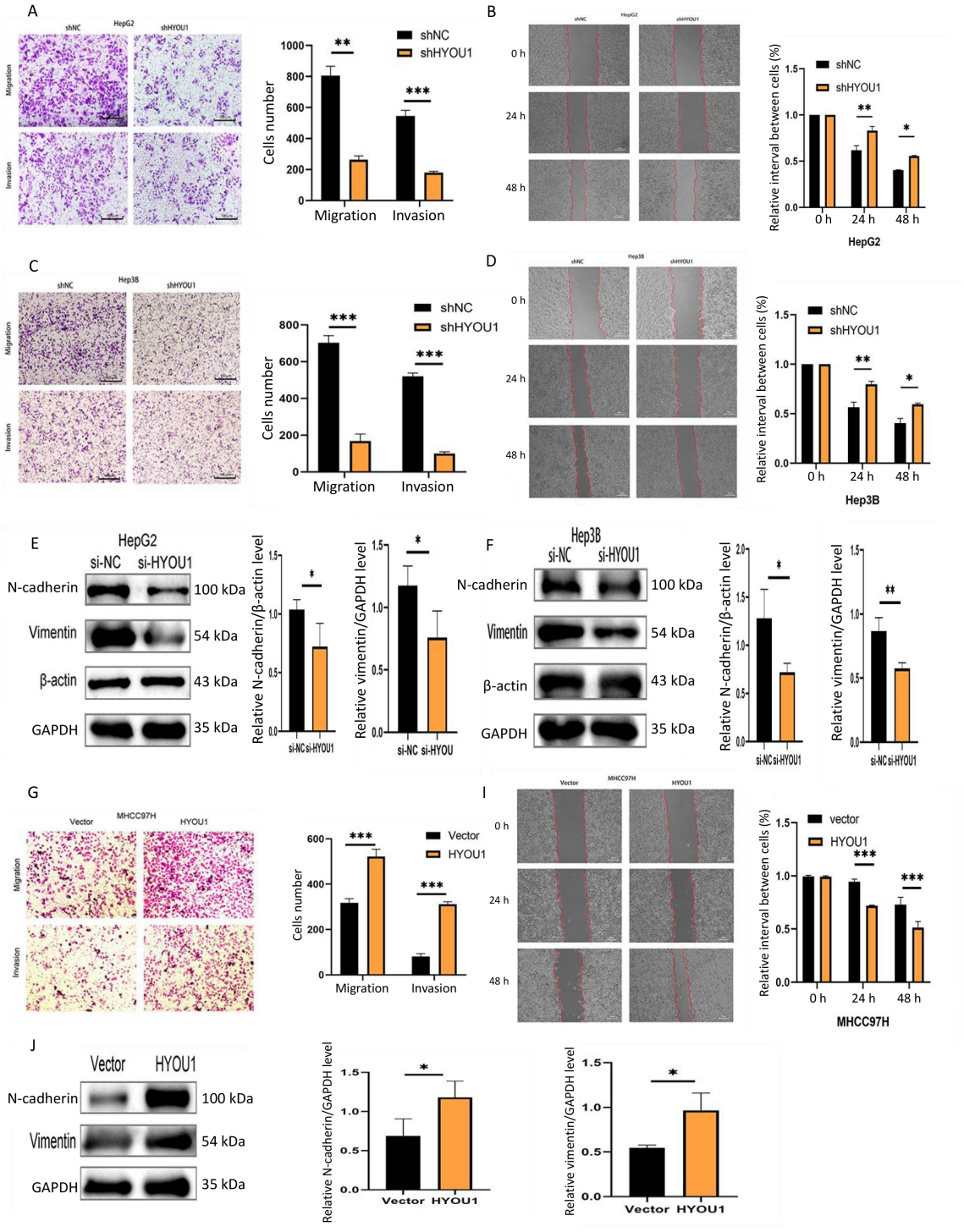

Fig. 5 HYOU1 promotes liver cancer cell invasion and migration. (A, B) Detecting the effects of *HYOU1* knockdown on the migration and invasion of HepG2 cells by Transwell and wound healing assays. (C, D) Decting the effects of *HYOU1* knockdown on the migration and invasion abilities of Hep3B cells by Transwell and wound healing assays. (E, F) WB analysis of N-cadherin and vimentin protein expression after HYOU1 knockdown in HepG2 and Hep3B cells. (G, H) Transwell and wound healing assays to assess the effects of HYOU1 overexpression. (I) WB analysis of N-cadherin and vimentin protein expression following HYOU1 overexpression. WB, Western blotting.

significantly upregulated and 631 downregulated (Fig. 6A). Gene Ontology (GO) enrichment analysis indicated that these DEGs were linked to biological processes, including extracellular matrix organization, composition of the extracellular matrix, and activity of potassium ion transmembrane transporters (Fig. 6B). Moreover, Kyoto Encyclopedia of Genes and Genomes (KEGG) pathway analysis revealed that these DEGs were

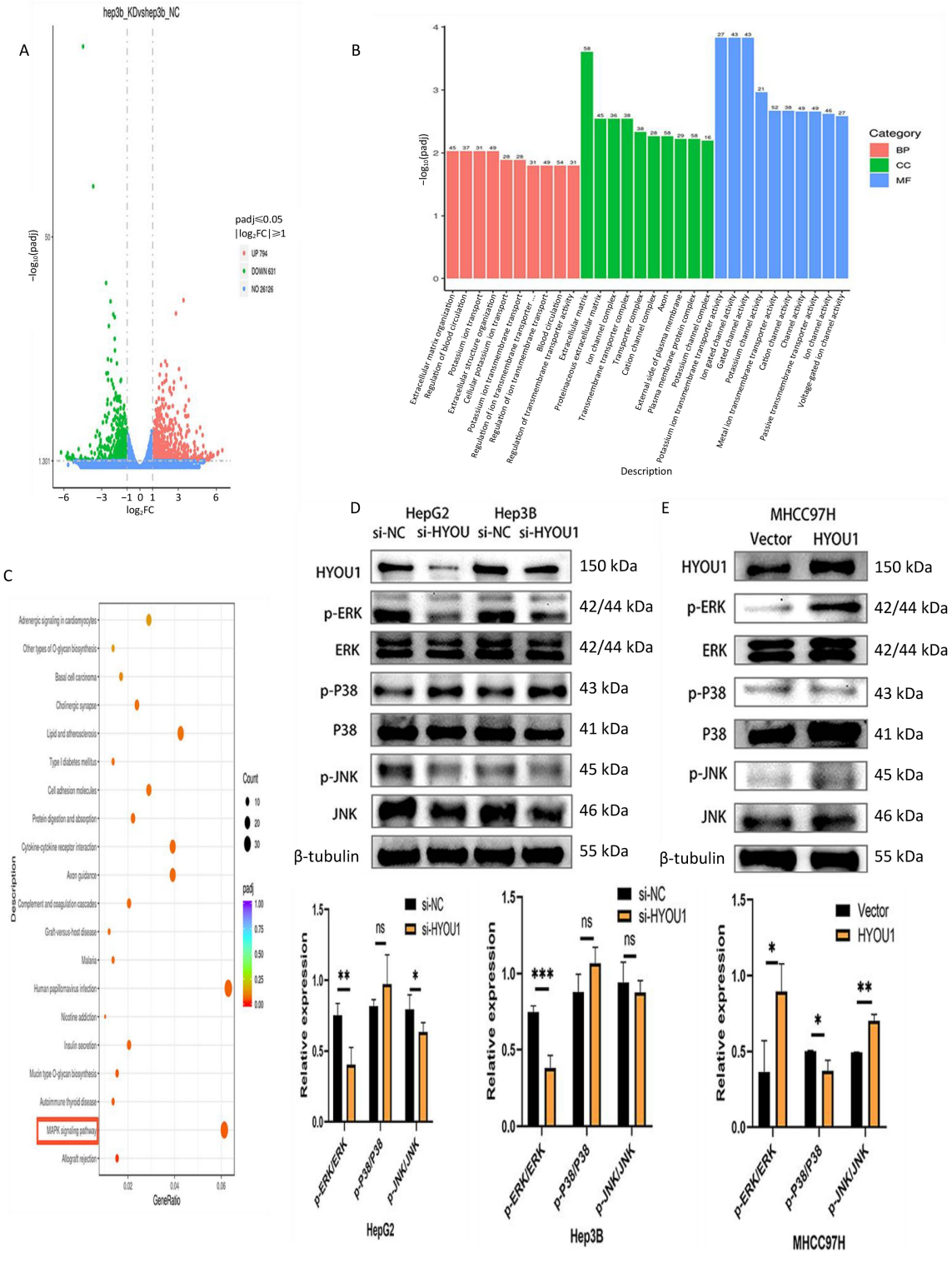

Fig. 6 HYOU1 activates the ERK/MAPK pathway. (A) Volcano plot of DEGs following *HYOU1* knockdown. (B) Bar chart of GO enrichment analysis. (C) Bubble plot of KEGG enrichment analysis. (D) WB analysis of MAPK pathway-related protein expression after *HYOU1* knockdown. (E) WB analysis of MAPK pathway-related protein expression after HYOU1 overexpression. KEGG, Kyoto Encyclopedia of Genes and Genomes; WB, Western blotting. Statistical significance: ns, not significant; *$P < 0.05$, **$P < 0.01$, ***$P < 0.001$.

enriched in pathways such as MAPK pathway, human papillomavirus infection, lipid metabolism, and atherosclerosis (Fig. 6C). Previous research has shown that abnormalities in MAPK pathway, which plays a crucial role in survival, tumor growth, metastasis, invasion, and angiogenesis, are strongly associated with

cancer development [16]. Building on our previous results, which demonstrated that HYOU1 enhances liver cancer cell proliferation, migration, and invasion while suppressing apoptosis, we speculated that the oncogenic role of HYOU1 might be mediated via the activation of the MAPK pathway. To determine whether HYOU1 affects liver cancer progression via the MAPK pathway, we conducted WB analysis to examine the expression of key downstream proteins. These findings indicated that silencing HYOU1 resulted in reduced levels of phosphorylated ERK (p-ERK) and phosphorylated JNK, whereas phosphorylated p38 expression was elevated (Fig. 6D). Conversely, HYOU1 overexpression had the opposite effect (Fig. 6E).

Since p-ERK/ERK exhibited the most prominent changes, we investigated the ERK/MAPK pathway. Using U0126, a specific ERK pathway inhibitor, we observed that U0126 significantly reduced p-ERK and Bcl-2 protein expression while upregulating Bax (Fig. 7A). Moreover, compared to HYOU1 knockdown alone, the combination of HYOU1 knockdown and U0126 treatment further suppressed liver cancer cell proliferation ($P < 0.05$) (Fig. 7B and 7C). Flow cytometry analysis demonstrated that U0126 inhibition of the ERK pathway further increased apoptosis in liver cancer cells ((DMSO + si-NC) : (DMSO + si-HYOU1) = (11.12 ± 0.57) : (24.42 ± 2.33), $P < 0.01$; (DMSO + si-HYOU1) : (si-HYOU + U0126) = (24.42 ± 2.33) : (33.51 ± 1.56), $P < 0.01$) (Fig. 7D). These results suggest that HYOU1 could influence the proliferation and apoptosis of liver cancer cells by modulating the ERK/MAPK pathway.

ERS promotes lenvatinib resistance in liver cancer

ERS has been linked to the development of resistance to different cancer treatments. To investigate whether ERS

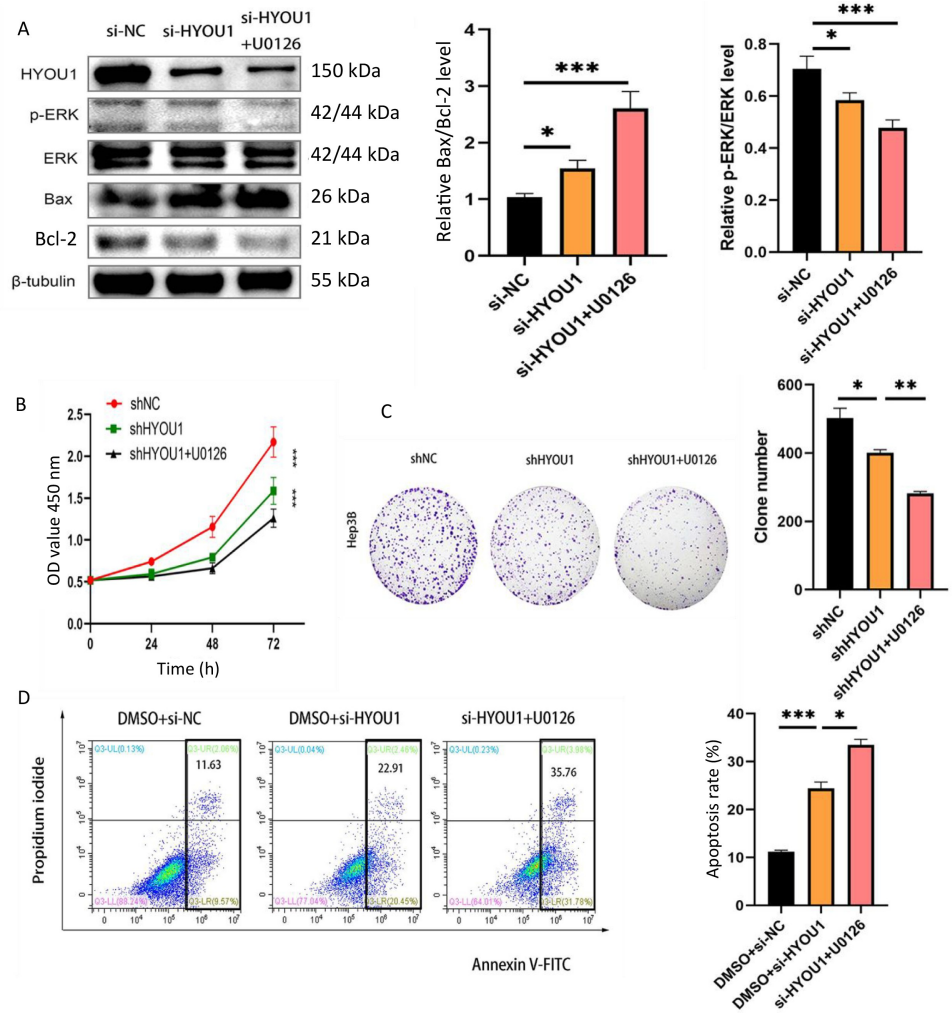

Fig. 7 HYOU1 activates the ERK/MAPK pathway to mediate liver cancer proliferation and apoptosis. (A) WB analysis of p-ERK, ERK, Bax, and Bcl-2 protein expression following the ERK pathway inhibitor U0126. (B, C) Proliferative capacity of liver cancer cells after U0126 treatment is assessed using CCK-8 and colony formation assays. (D) Flow cytometry analysis of apoptosis in cells following U0126 treatment. WB, Western blotting. Statistical significance: *$P < 0.05$, **$P < 0.01$, ***$P < 0.001$.

contributes to lenvatinib resistance, we first employed the CCK-8 assay to assess the impact of lenvatinib on the proliferation of liver cancer cells. The findings indicated a gradual decline in Hep3B and HepG2 cell viability with increasing lenvatinib concentrations (Fig. 8A), and the IC_{50} was determined to be 11.42 μmol/L (Fig. 8B). Subsequently, HepG2 and Hep3B cells were treated with lenvatinib at concentrations of 5, 10, and 20 μmol/L for 24 and 48 h to assess how ERS influences the sensitivity of the cells to lenvatinib. The results demonstrated that ERS significantly reduced the lenvatinib-induced inhibition of liver cancer cell proliferation (Fig. 8C and 8D), suggesting that ERS may contribute to lenvatinib resistance. To validate this finding, flow cytometry was performed to assess apoptosis. The results revealed that ERS induction decreased lenvatinib-induced apoptosis in liver cancer cells, whereas treatment with 4-PBA, an ERS inhibitor, effectively reversed this effect of ERS induction. Moreover, the combination of 4-PBA and lenvatinib further enhanced apoptosis compared with lenvatinib treatment alone (Fig. 8E). These results indicate that ERS is a key factor contributing to lenvatinib resistance in liver cancer cells and suggest that inhibition of ERS could potentially improve the therapeutic effectiveness of lenvatinib.

Inhibition of HYOU1 reverses ERS-related lenvatinib resistance

ERS is a key factor that contributes to tumor cell resistance to apoptosis. However, it remains unclear whether ERS influences lenvatinib sensitivity in liver cancer cells by regulating HYOU1 expression. To address this, we knocked down *HYOU1* expression in liver cancer cells using siRNA and subsequently treated the cells with lenvatinib. Flow cytometric analysis demonstrated that HYOU1 knockdown significantly enhanced lenvatinib-induced apoptosis ($P < 0.01$) (Fig. 9A). To explore the effect of HYOU1 expression on lenvatinib sensitivity, we developed a subcutaneous xenograft model using BALB/c mice and subjected them to lenvatinib treatment. The results showed that tumors in the shHYOU1 +

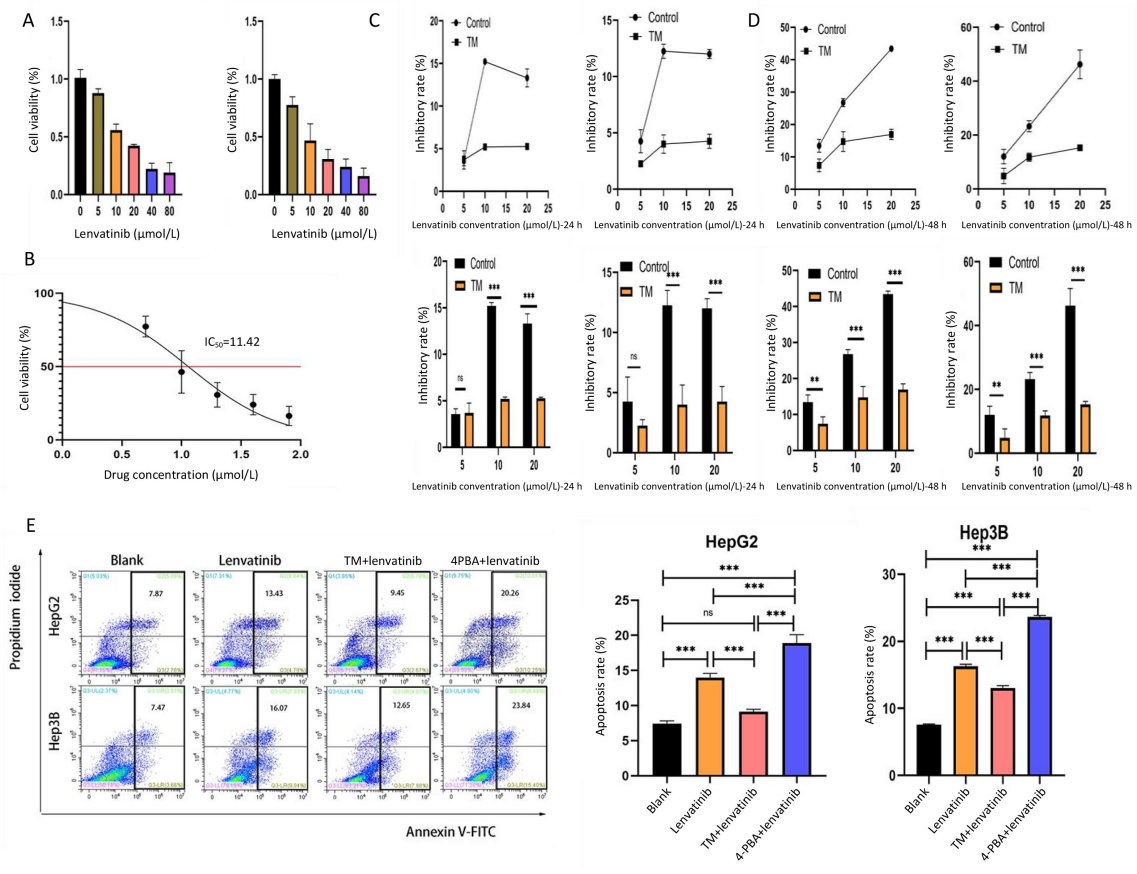

Fig. 8 ERS induces lenvatinib resistance. (A) Proliferation capacity of HepG2 and Hep3B treated with different concentrations of lenvatinib. (B) Determination of the IC_{50} value of lenvatinib. (C, D) TM-induced ERS diminishes the suppressive impact of lenvatinib on HepG2 and Hep3B cells following 24 and 48 h of treatment with lenvatinib in 5, 10, and 20 μmol/L. (E) Apoptosis rates of liver cancer cells under various treatment conditions as analyzed by flow cytometry. ERS, endoplasmic reticulum stress; TM, tunicamycin. Statistical significance: $*P < 0.05$, $**P < 0.01$, $***P < 0.001$.

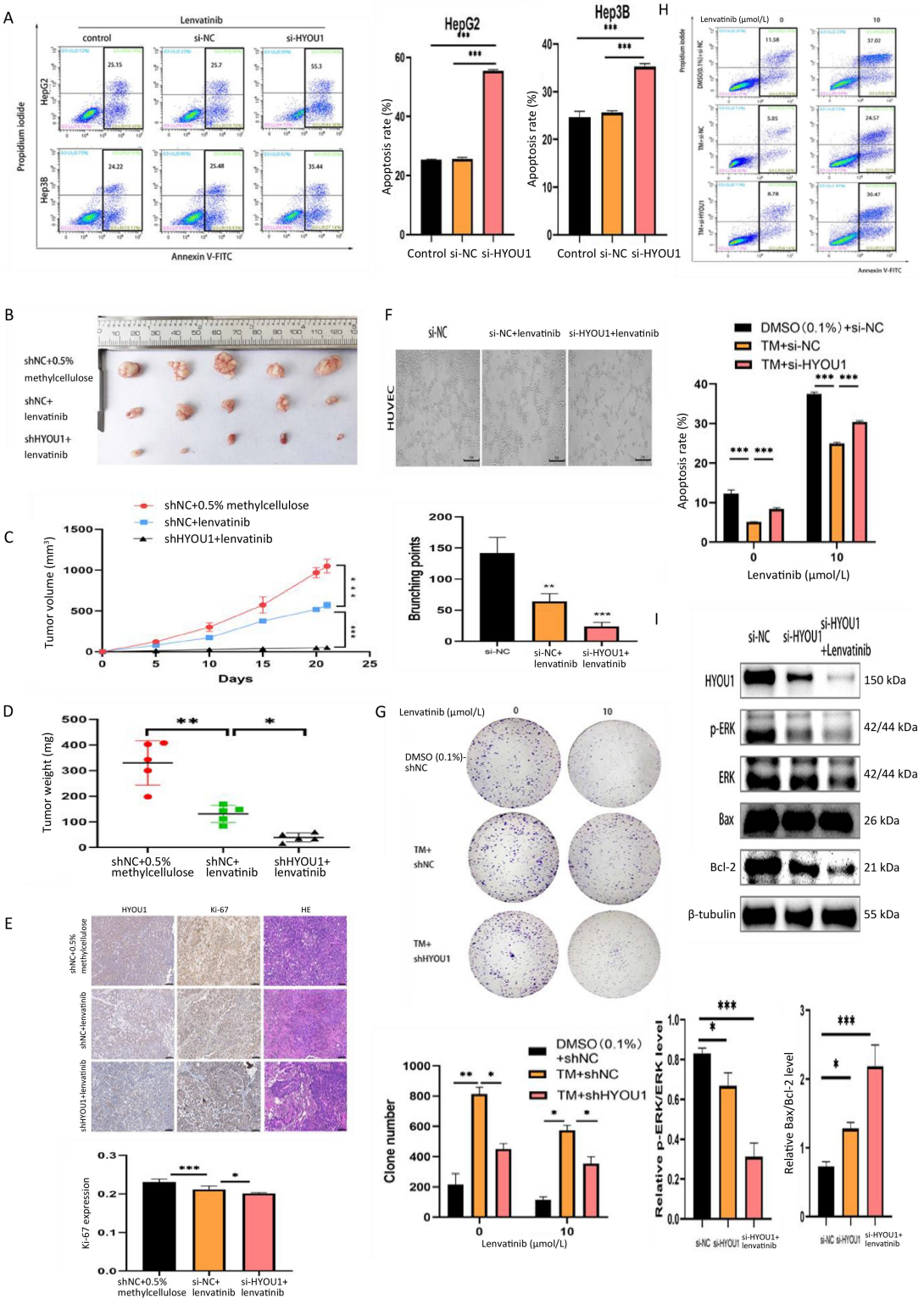

Fig. 9 HYOU1 inhibition partially reverses ERS-induced lenvatinib resistance. (A) Flow cytometry analysis of liver cancer cell sensitivity to lenvatinib upon HYOU1 downregulation. (B) Representative photographs of tumor-bearing mice from various treatment groups following drug administration. (C) Tumor volume and (D) tumor weight are subsequently measured. (E) Immunohistochemistry staining of xenograft tumors from each group revealed expression levels of HYOU1 and Ki-67 (scale bar: 100 μm). (F) Angiogenesis assay confirmed the inhibition of *HYOU1* knockdown and lenvatinib on angiogenesis. (G, H) Assessing cell proliferation and apoptosis in liver cancer cells subjected to different treatment conditions by CCK-8 and flow cytometry. (I) Role of the ERK/MAPK pathway in contributing to resistance against lenvatinib. ERS, endoplasmic reticulum stress; TM, tunicamycin. Statistical significance: $^{*}P < 0.05$, $^{**}P < 0.01$, $^{***}P < 0.001$.

lenvatinib group were significantly smaller compared to those in the other two groups (Fig. 9B), with a marked decrease in both tumor volume ($P < 0.01$) (Fig. 9C) and weight ($P < 0.05$) (Fig. 9D). IHC staining of tumor samples indicated a notable reduction in the Ki-67 proliferation index in the shHYOU1 + lenvatinib group compared to that in the control group (Fig. 9E), suggesting that HYOU1 inhibition enhances the therapeutic effect of lenvatinib. To investigate the effects of lenvatinib and HYOU1 on angiogenesis, we performed angiogenesis assays. The results showed that lenvatinib inhibited angiogenesis, and the combination of HYOU1 knockdown and lenvatinib further suppressed angiogenesis (Fig. 9F). To further verify whether HYOU1 is involved in ERS-mediated lenvatinib resistance, we performed colony formation assays and flow cytometry to evaluate changes in lenvatinib sensitivity in liver cancer cells under ERS. These findings revealed that ERS activation partially mitigated the suppressive effect of HYOU1 knockdown on tumor cell growth (Fig. 9G) and reduced the increase in apoptosis (Fig. 9H). Additionally, we explored the role of the HYOU1-mediated ERK/MAPK pathway in lenvatinib resistance. WB analysis revealed that HYOU1 knockdown combined with lenvatinib treatment significantly reduced p-ERK expression (Fig. 9I), indicating that HYOU1 influences lenvatinib resistance by modulating the ERK/MAPK pathway.

Discussion

Emerging research has demonstrated that ERS plays a crucial role in tumor progression and therapeutic resistance. This process may be driven by various mechanisms, including angiogenesis, autophagy, EMT, energy metabolism reprogramming, and chemical modification of mRNA. Previous studies indicate that DEGs in ERS may be subject to regulatory control, contributing to disease progression [17] and ERS-associated drug resistance [18]. However, the mechanisms by which DEGs under ERS regulate apoptosis resistance, promote tumor progression, and contribute to therapeutic resistance in liver cancer remain unclear.

We performed RNA-seq and proteomic sequencing analyses on both the ERS and control models, revealing that ERS regulates HYOU1. HYOU1, also called ORP150 or GRP170, is a member of the HSP70 protein family and is rich in CCAAT cis-regulatory elements. Additionally, it features a typical HSP70 structural framework comprising a helical domain at the C terminus and an N-terminal nucleotide binding domain [19]. This structural composition facilitates the linkage between ATP hydrolysis and substrate protein binding and release, playing a crucial role in preserving ER protein homeostasis. Previous studies have shown that HYOU1 expression is upregulated under various conditions, including ischemia [20], hypoxia [21], and ERS induced by TM. ERS activates three classical UPR pathways, which subsequently stimulate transcriptional programs that enhance the expression of ER chaperones: X-box binding protein 1, GRPs, and components of ER-associated degradation (ERAD), aiding in the removal of misfolded proteins [22]. Upregulation of molecular chaperones within the ER, including GRP170 (a widely recognized marker of the UPR), aids in reducing protein overload and reestablishing ER equilibrium [23]. Whole-genome analysis of TM-induced ERS in neonatal rat cardiomyocytes by Liu *et al*. confirmed that HYOU1 expression was upregulated upon TM treatment [24]. Similarly, Inagi *et al*. demonstrated that the treatment of podocytes with TM, A23187, and SNAP upregulated the expression of ERS-associated chaperones, including HYOU1 and GRP78. Their study provided further evidence that ERS and the upregulation of ERS proteins (e.g., ORP150 and GRP78) were linked to megsin transgenic rat podocytes [25]. Our findings confirmed that ERS upregulated HYOU1 expression in liver cancer cells. Based on previous research, we hypothesized that this regulation might be related to the nucleotide exchange function of HYOU1 [26]. When proteins undergo misfolding in the ER, they are degraded via the ERAD pathway. HYOU1 facilitates the recruitment and activation of GRP78 nucleotide exchange, converting ADP-GRP78 to ATP-GRP78, which then undergoes conformational changes, releases its substrate, and enables misfolded proteins to be transported into the cytosol for degradation, thereby maintaining protein homeostasis [27]. These studies provide substantial evidence that ERS leads to the upregulation of HYOU1.

Earlier research has shown that HYOU1 is functionally involved in the development and progression of multiple diseases. Elevated HYOU1 expression has been reported in bladder cancer [28], nasopharyngeal carcinoma [29], and other cancers. To investigate the precise mechanism by which HYOU1 exerts its effects, we successfully established a stable HYOU1-knockdown Hep3B cell line. The DEGs were overrepresented in the MAPK pathway. Further experimental validation confirmed that the ERK/MAPK pathway is the primary signaling mechanism activated by HYOU1. This study is the first to demonstrate that HYOU1 enhances liver cancer malignancy by activating the ERK/MAPK pathway. Previous studies have emphasized the involvement of the ERK/MAPK pathway in tumor progression [30]. For example, in ovarian cancer, CSGALNACT2 regulates the ERK/MAPK pathway via DUSP1 to suppress cancer cell migration and invasion [31]. In this study, HYOU1 inhibition decreased p-ERK protein expression,

suppressed liver cancer cell proliferation, and increased apoptosis. These results imply that focusing on HYOU1 and the ERK/MAPK pathway may offer new therapeutic strategies for liver cancer. If confirmed in clinical trials, this approach may offer new perspectives for the treatment and management of this disease.

Numerous studies have confirmed that genes associated with ERS play important roles in tumor treatment resistance. Previous research has demonstrated a co-expression relationship between HYOU1 and VEGF [32,33], leading us to hypothesize that HYOU1 is involved in ERS-induced resistance to lenvatinib. Although lenvatinib has significant therapeutic value for patients with liver cancer, many patients fail to benefit due to the development of drug resistance. Recent studies have shown that targeting specific molecules can reverse lenvatinib resistance in liver cancer. For example, Guo *et al*. found that KDM6A plays a critical role in lenvatinib resistance by upregulating FGFR4 expression [34]. Our results show that downregulation of HYOU1 can partially reverse ERS-induced lenvatinib resistance by promoting apoptosis and inhibiting proliferation of liver cancer cells. Additionally, we found that both HYOU1 knockdown and lenvatinib treatment suppress angiogenesis, possibly through inhibition of the ERK/MAPK pathway. Targeting HYOU1 and the ERK/MAPK pathway may represent a potential strategy to overcome lenvatinib resistance in liver cancer. These findings may provide valuable clinical insights for developing therapeutic strategies against lenvatinib resistance.

In conclusion, our study demonstrates, for the first time, the critical role of HYOU1 in liver cancer progression, suggesting that its function may be associated with ERK/MAPK pathway activation and ERS regulation. Our findings indicate that HYOU1 inhibition may partially reverse ERS-induced lenvatinib resistance, offering new insights and potential therapeutic strategies for liver cancer pathogenesis and treatment. However, given the complexity of tumor development, whether HYOU1 contributes to liver cancer progression through additional mechanisms, and what the precise role of HYOU1 is in reversing lenvatinib resistance. Due to limited conditions, our prognostic analysis was conducted on only 29 patients, which inevitably imposes certain limitations. In future studies, pending availability of multi-center data, we plan to perform survival analyses related to HYOU1 expression to enhance the scientific rigor and reliability of our findings. These questions warrant further investigation.

Acknowledgements

This study was supported by the National Natural Science Foundation of China (Nos. 82072751 and 82072687) and the Institute of Pharmacology, Anhui Medical University.

Compliance with ethics guidelines

Conflicts of interest Xiao Du, Weijia Jiang, Sitong Yan, Xiang Chen, Anqi Wang, Jiatao Liu, Lulu Fan, Yuhan Huang, Xiangyu Zu, and Guoping Sun declare no conflicts of interest.

The study was approved by the First Affiliated Hospital of Anhui Medical University (No. 20200931) and the study was performed in accordance with the ethical standards as laid down in the 1964 Declaration of Helsinki and its later amendments or comparable ethical standards. Informed consent was obtained from all patients for being included in the study. The Animal Ethics Committee of the Anhui Medical University (No. 20242232) approved all animal studies.

Electronic supplementary material Supplementary material is available in the online version of this article at https://doi.org/10.1007/s11684-025-1173-z and is accessible for authorized users.

References

1. Siegel RL, Giaquinto AN, Jemal A. Cancer statistics, 2024. CA Cancer J Clin 2024; 74(1): 12–49
2. Rumgay H, Arnold M, Ferlay J, Lesi O, Cabasag CJ, Vignat J, Laversanne M, McGlynn KA, Soerjomataram I. Global burden of primary liver cancer in 2020 and predictions to 2040. J Hepatol 2022; 77(6): 1598–1606
3. Forner A, Reig M, Bruix J. Hepatocellular carcinoma. Lancet 2018; 391(10127): 1301–1314
4. Ajoolabady A, Kaplowitz N, Lebeaupin C, Kroemer G, Kaufman RJ, Malhi H, Ren J. Endoplasmic reticulum stress in liver diseases. Hepatology 2023; 77(2): 619–639
5. Akman M, Belisario DC, Salaroglio IC, Kopecka J, Donadelli M, De Smaele E, Riganti C. Hypoxia, endoplasmic reticulum stress and chemoresistance: dangerous liaisons. J Exp Clin Cancer Res 2021; 40(1): 28
6. Wang DQ, Miao XJ, Gao J, Zhou Y, Ji F, Cheng X. The 150-kDa oxygen-regulated protein (ORP150) regulates proteinuria in diabetic nephropathy via mediating VEGF. Exp Mol Pathol 2019; 110: 104255

7. Tamatani M, Matsuyama T, Yamaguchi A, Mitsuda N, Tsukamoto Y, Taniguchi M, Che YH, Ozawa K, Hori O, Nishimura H, Yamashita A, Okabe M, Yanagi H, Stern DM, Ogawa S, Tohyama M. ORP150 protects against hypoxia/ischemia-induced neuronal death. Nat Med 2001; 7(3): 317–323
8. Kitao Y, Hashimoto K, Matsuyama T, Iso H, Tamatani T, Hori O, Stern DM, Kano M, Ozawa K, Ogawa S. ORP150/HSP12A regulates purkinje cell survival: a role for endoplasmic reticulum stress in cerebellar development. J Neurosci 2004; 24(6): 1486–1496
9. Hao A, Wang Y, Zhang X, Li J, Li Y, Li D, Kulik G, Sui G. Long non-coding antisense RNA HYOU1-AS is essential to human breast cancer development through competitive binding hnRNPA1 to promote HYOU1 expression. Biochim Biophys Acta Mol Cell Res 2021; 1868(4): 118951
10. Wang W, Jiang X, Xia F, Chen X, Li G, Liu L, Xu Q, Zhu M, Chen C. HYOU1 promotes cell proliferation, migration, and invasion via the PI3K/AKT/FOXO1 feedback loop in bladder cancer. Mol Biol Rep 2023; 50(1): 453–464
11. Zhou Y, Liao Q, Li X, Wang H, Wei F, Chen J, Yang J, Zeng Z, Guo X, Chen P, Zhang W, Tang K, Li X, Xiong W, Li G. HYOU1, regulated by LPLUNC1, is up-regulated in nasopharyngeal carcinoma and associated with poor prognosis. J Cancer 2016; 7(4): 367–376
12. Abu El-asrar AM, Ahmad A, Alam K, Bittoun E, Siddiquei MM, Mohammad G, Mousa A, De Hertogh G, Opdenakker G. Association of 150-kDa oxygen-regulated protein with vascular endothelial growth factor in proliferative diabetic retinopathy. Acta Ophthalmol 2018; 96(4): e460–e467
13. Gujarathi R, Franses JW, Pillai A, Liao CY. Targeted therapies in hepatocellular carcinoma: past, present, and future. Front Oncol 2024; 14: 1432423
14. Wang J, Yu H, Dong W, Zhang C, Hu M, Ma W, Jiang X, Li H, Yang P, Xiang D. N^6-methyladenosine-mediated up-regulation of FZD10 regulates liver cancer stem cells' properties and lenvatinib resistance through WNT/β-catenin and hippo signaling pathways. Gastroenterology 2023; 164(6): 990–1005
15. Hu B, Zou T, Qin W, Shen X, Su Y, Li J, Chen Y, Zhang Z, Sun H, Zheng Y, Wang CQ, Wang Z, Li TE, Wang S, Zhu L, Wang X, Fu Y, Ren X, Dong Q, Qin LX. Inhibition of EGFR overcomes acquired lenvatinib resistance driven by STAT3–ABCB1 signaling in hepatocellular carcinoma. Cancer Res 2022; 82(20): 3845–3857
16. Ullah R, Yin Q, Snell AH, Wan L. RAF-MEK-ERK pathway in cancer evolution and treatment. Semin Cancer Biol 2022; 85: 123–154
17. Zhu Y, Cui J, Liu J, Hua W, Wei W, Sun G. Sp2 promotes invasion and metastasis of hepatocellular carcinoma by targeting TRIB3 protein. Cancer Med 2020; 9(10): 3592–3603
18. Akman M, Belisario DC, Sailaroglio IC, Kopecka J, Donadelli M, De Smaele E, Riganti C. Hypoxia, endoplasmic reticulum stress and chemoresistance: dangerous liaisons. J Exp Clin Cancer Res 2021; 40(1): 28
19. Pagare PP, Wang H, Wang XY, Zhang Y. Understanding the role of glucose regulated protein 170 (GRP170) as a nucleotide exchange factor through molecular simulations. J Mol Graph Model 2018; 85: 160–170
20. Kitano H, Nishimura H, Tchibana H, Yoshikawa H, Matsuyama T. ORP150 ameliorates ischemia/reperfusion injury from middle cerebral artery occlusion in mouse brain. Brain Res 2004; 1015(1–2): 122–128
21. Ozawa K, Kuwabar K, Tamatani M, Takatsuji K, Tsukamoto Y, Kaneda S, Yanagi H, Stern DM, Eguchi Y, Tsujimoto Y, Ogawa S, Tohyama M. 150-kDa oxygen-regulated protein (ORP150) suppresses hypoxia-induced apoptotic cell death. J Biol Chem 1999; 274(10): 6397–6404
22. Wang H, Pezeshki AM, Yu X, Guo C, Subjeck JR, Wang XY. The endoplasmic reticulum chaperone GRP170: from immunobiology to cancer therapeutics. Front Oncol 2015; 4: 377
23. Rutkowski DT, Hegde RS. Regulation of basal cellular physiology by the homeostatic unfolded protein response. J Cell Biol 2010; 189(5): 783–794
24. Liu CL, Zhong W, He YY, Li X, Li S, He KL. Genome-wide analysis of tunicamycin-induced endoplasmic reticulum stress response and the protective effect of endoplasmic reticulum inhibitors in neonatal rat cardiomyocytes. Mol Cell Biochem 2016; 413(1–2): 57–67
25. Inagi R, Nangaku M, Onogi H, Ueyama H, Kitao Y, Nakazato K, Ogawa S, Kurokawa K, Couser WG, Miyata T. Involvement of endoplasmic reticulum (ER) stress in podocyte injury induced by excessive protein accumulation. Kidney Int 2005; 68(6): 2639–2650
26. Behnke J, Feige MJ, Hendershot LM. BiP and its nucleotide exchange factors Grp170 and Sil1: mechanisms of action and biological functions. J Mol Biol 2015; 427(7): 1589–1608
27. Inoue T, Tsai B. The Grp170 nucleotide exchange factor executes a key role during ERAD of cellular misfolded clients. Mol Biol Cell 2016; 27(10): 1650–1662
28. Wang W, Jiang X, Xia F, Chen X, Li G, Liu L, Xu Q, Zhu M, Chen C. HYOU1 promotes cell proliferation, migration, and invasion via the PI3K/AKT/FOXO1 feedback loop in bladder cancer. Mol Biol Rep 2023; 50(1): 453–464
29. Lee M, Song Y, Choi I, Lee SY, Kim S, Kim SH, Kim J, Seo HR. Expression of HYOU1 via reciprocal crosstalk between NSCLC cells and HUVECs control cancer progression and chemoresistance in tumor spheroids. Mol Cells 2021; 44(1): 50–62
30. Wang JM, Jiang JY, Zhang DL, Du X, Wu T, Du ZX. HYOU1 facilitates proliferation, invasion and glycolysis of papillary thyroid cancer via stabilizing LDHB mRNA. J Cell Mol Med 2021; 25(10): 4814–4825
31. Ma M, Wang C, Wu M, Gu S, Yang J, Zhang Y, Cheng S, Xu S, Zhang M, Wu Y, Zhao Y, Tian X, Voon DCC, Takahashi C, Sheng J, Wang Y. CSGALNACT2 restricts ovarian cancer migration and invasion by modulating MAPK/ERK pathway through DUSP1. Cell Oncol (Dordr) 2024; 47(3): 897–915
32. Ozawa K, Kondo T, Hori O, Kitao Y, Stern DM, Eisenmenger W, Ogawa S, Ohshima T. Expression of the oxygen-regulated protein ORP150 accelerates wound healing by modulating intracellular VEGF transport. J Clin Invest 2001; 108(1): 41–50
33. Abu El-Asrar AM, Ahmad A, Alam K, Bittoun E, Siddiquei MM, Mohammad G, Mousa A, De Hertogh G, Opdenakker G. Association of 150-kDa oxygen-regulated protein with vascular endothelial growth factor in proliferative diabetic retinopathy. Acta Ophthalmol 2018; 96(4): e460–e467
34. Guo W, Li S, Qian Y, Li L, Wang F, Tong Y, Li Q, Zhu Z, Gao WQ, Liu Y. KDM6A promotes hepatocellular carcinoma progression and dictates lenvatinib efficacy by upregulating FGFR4 expression. Clin Transl Med 2023; 13(10): e1452